more negative is caused by the enhanced adsorption of the cationic forms at negative potentials. In accord with earlier studies of similar compounds, the protonated forms appear to adsorb in association with halide ions.

This study shows that near pH 7, both the neutral free aldehyde (the reducible form) and the neutral hydrate are adsorbed. However, for $1 < pH < 4$, most of the adsorbed aldehyde is protonated (Figure 3), and, consequently, very little free aldehyde is present. Nevertheless, the reduction reaction is not impeded. In separate experiments, we found that diffusion-controlled reduction of the free aldehyde was observed by chronoamperometry at pH 3.86 and 6.88 at both silver and mercury electrodes. We conclude that either the reactant need not adsorb before the reduction occurs or, if it must adsorb, this step is not rate-limiting.

Acknowledgment. This research was supported by the National Science Foundation (Grant CHE-8722764).

Registry No. 4-Pyridinecarboxaldehyde, 872-85-5; silver, 7440-22-4; chloride, 16887-00-6; bromide, 24959-67-9; iodide, 20461-54-5; protonated 4-pyridinecarboxaldehyde hydrate, 105868-55-1.

Resonance Raman Studies of Hydrogenase-Catalyzed Reduction of Cytochrome c_3 by Hydrogen. Evidence for Heme–Heme Interactions

A. L. Verma,[1a] K. Kimura, A. Nakamura,[1b] T. Yagi,[1c] H. Inokuchi, and T. Kitagawa*,†

Contribution from the Institute for Molecular Science, Okazaki National Research Institutes, Myodaiji, Okazaki 444, Japan. *Received September 14, 1987*

Abstract: We observed splittings of Raman bands for a multi-heme protein for the first time. In the resonance Raman studies of hydrogenase-catalyzed reduction of a tetraheme protein cytochrome c_3 (Cyt-c_3) with hydrogen, certain Raman bands show clear splittings in the intermediate redox states obtained under controlled pressure of hydrogen, while apparently nonstructured bands were observed in the fully oxidized or fully reduced states. This suggests either nonequivalence in the environments of the four hemes or an exciton-like splitting of vibrational modes. Since various C-type cytochromes at neutral pH, which have different amino acid compositions but the same axial ligands, do not give a wide variety of frequencies for a given mode and, furthermore, a bandwidth of the Soret band was much narrower with Cyt-c_3 than with various single-heme cytochromes c, it is more likely to assume that the four hemes in the protein interact directly with each other, giving rise to exciton-like splitting. Observation of well-defined Raman lines in the partially reduced states at the characteristic frequencies for the reduced or the oxidized form indicates that the electron-exchange rate, either intramolecular within the four hemes or intermolecular between different Cyt-c_3 molecules, is much slower than the time scale of the RR scattering process while the recent NMR studies indicate that the intramolecular electron-exchange rates are faster than 10^9 s^{-1}. We have attempted to estimate the relative importance of the dispersion, induction, orientational, and repulsive interactions for understanding the splitting of the Raman bands. The dipole–dipole coupling mechanism can be ruled out while the dispersion-type interactions may contribute predominantly to it.

Cytochromes c_3 (Cyt-c_3), which are found in the strictly anaerobic sulfate reducing bacteria belonging to the genus *Desulfovibrio*, constitute a class of proteins containing four C-type hemes bound covalently to a single polypeptide with $M_r = 13\,000$. All four heme irons in each molecule are coordinated by two histidine residues, adopting the hexacoordinated low-spin form in both the oxidized and reduced states of the protein. Physiologically Cyt-c_3 acts as an electron carrier of *Desulfovibrio* hydrogenase (hydrogen:ferricytochrome c_3 oxidoreductase, EC 1.12.2.1)[2] and plays a key role in the complex sulfate reduction metabolism of *Desulfovibrio*. This protein is very interesting since the anhydrous solid film of its reduced form on a quartz plate exhibits almost metallic conductivity in magnitude and there is a 10^{13}-fold difference in the electrical resistivity between the oxidized and reduced forms.[3a-c]

The physicochemical properties of the five varieties of Cyt-c_3 from different species in the genus *Desulfovibrio* have been investigated by several groups using optical absorption,[2,4,5] nuclear magnetic resonance,[6,7] electron spin resonance,[8,9] Mössbauer,[10] electrical conductivity,[3] ionization potentials,[11] and electrochemical[12,13] techniques (see ref 13 for a review). One of the peculiar features of the Cyt-c_3 is its very negative redox potential and it can be reduced by hydrogen in the presence of hydrogenase. The electrochemical,[4] NMR,[6,7] and ESR[9] studies suggest that the Cyt-c_3 accepts four electrons in a stepwise manner and the different redox states are characterized by four separate but closely spaced negative redox potentials. Recent X-ray diffraction studies[14,15] on the two species of Cyt-c_3 show that the relative disposition of

† Author to whom reprint requests should be addressed.

(1) (a) Permanent address: Department of Physics, North-Eastern Hill University, Shillong-793003, India. (b) Central Research Laboratories, Ajinomoto Co., Inc., Suzuki-cho, Kawasaki 210, Japan. (c) Department of Chemistry, Shizuoka University, Oya, Shizuoka 422, Japan.

(2) (a) Yagi, T.; Maruyama, K. *Biochim. Biophys. Acta* **1971**, *243*, 214. (b) Yagi, T.; Honya, M.; Tamiya, N. *Biochim. Biophys. Acta* **1968**, *153*, 699.

(3) (a) Kimura, K.; Nakahara, Y.; Yagi, T.; Inokuchi, H. *J. Chem. Phys.* **1979**, *70*, 3317. (b) Nakahara, Y.; Kimura, K.; Inokuchi, H.; Yagi, T. *Chem. Phys. Lett.* **1980**, *73*, 31. (c) Ichimura, K.; Kimura, K.; Nakahara, Y.; Yagi, T.; Inokuchi, H. *Chem. Lett.* **1982**, 19.

(4) Druker, H.; Campbell, L. L.; Woody, R. W. *Biochemistry* **1970**, *9*, 1519.

(5) Meyer, T. E.; Bartsch, R. G.; Kamen, M. D. *Biochim. Biophys. Acta* **1971**, *245*, 453.

(6) (a) Dobson, C. M.; Hoyle, N. J.; Geraldes, C. F.; Wright, P. E.; Williams, R. J. P.; Bruschi, M.; LeGall, J. *Nature (London)* **1974**, *249*, 425. (b) McDonald, C. C.; Phillips, W. D.; LeGall, J. *Biochemistry* **1974**, *13*, 1952.

(7) (a) Fan, K.; Akutsu, H.; Niki, K.; Kyogoku, Y., to be published. (b) Kimura, K.; Nakajima, S.; Niki, K.; Inokuchi, H., unpublished data.

(8) DerVartanian, D. V. *J. Magn. Reson.* **1973**, *10*, 1.

(9) DerVartanian, D. V.; LeGall, J. *Biochim. Biophys. Acta* **1974**, *346*, 79.

(10) Utsuno, M.; Ono, K.; Kimura, K.; Inokuchi, H.; Yagi, T. *J. Chem. Phys.* **1980**, *72*, 2264.

(11) Kimura, K.; Sato, N.; Hino, S.; Yagi, T.; Inokuchi, H. *J. Am. Chem. Soc.* **1978**, *100*, 6564.

(12) Hinnen, C.; Parsons, R.; Niki, K. *J. Electroanal. Chem.* **1983**, *147*, 329.

(13) Yagi, T.; Inokuchi, H.; Kimura, K. *Acc. Chem. Res.* **1983**, *16*, 2.

(14) Haser, R.; Pierrot, M.; Frey, M.; Payan, F.; Astier, J. P.; Bruschi, M.; LeGall, J. *Nature (London)* **1979**, *282*, 806.

0002-7863/88/1510-6617$01.50/0

the four hemes in both species is similar but the orientation of the four hemes is asymmetric with respect to each other in each molecule. Although the distances between the heme irons range from 11 to 18 Å, some of the pyrrole atoms of hemes come very close to the nearby hemes due to their relative orientations. Because of this close proximity of the four heme units in Cyt-c_3, considerable direct interaction is expected between them, which may be responsible for some of the unusual properties such as low negative redox potential,[12] high electrical conductivity,[3b] and dependence of the microscopic redox potentials of individual hemes on the overall redox state.[7a] In spite of several studies, information about the electron-transfer rates, the nature of the interaction between the heme units, and the mechanism of the reduction process is still obscure on this system.

As the reduced and oxidized hemes have characteristic Raman features in different spectral regions and can be examined at physiologically relevant concentrations under resonance conditions, we have studied the hydrogenase-catalyzed reduction of Cyt-c_3 from *D. Vulgaris*, Miyazaki under controlled pressures of hydrogen using resonance Raman technique. We have observed splitting of many bands in the intermediate states of reduction and have discussed whether the band splitting arose from nonequivalent surroundings of four hemes or interheme interactions of equivalent hemes.

Experimental Procedures

Cytochrome c_3 and hydrogenase were isolated from sulfate-reducing bacteria (*Desulfovibrio vulgaris*, Miyazaki strain) and purified as per the reported procedure.[16a,b] Lyophilized Cyt-c_3 was dissolved in 4 mM phosphate buffer at pH 6.9 and a trace amount of hydrogenase was added to it. The concentration of the sample was determined from the known absorbance ($\epsilon_{mM}(\gamma) = 454.4$) for the oxidized form.[3a] Horse cytochrome *c* (Sigma type VI) was purified with the CM-52 column just before use.

In order to measure the RR spectra and monitor the absorption spectra before and after each run, a special cell was designed which could be evacuated to $\sim 10^{-5}$ Torr. Approximately a 10^{-4} M solution of Cyt-c_3 with a small amount of hydrogenase in 4 mM phosphate buffer (pH 6.9) was placed in the cell and evacuated thoroughly in repeated cycles without freezing the solution with a fore-pressure of 10^{-5} Torr. After thorough degassing, a known amount of hydrogen gas of 99.999% purity was introduced into the reaction cell and the pressure of the introduced hydrogen was monitored with a solid-state device (Fujikura Electric Wire Co., Tokyo).

The cell was shaken occasionally and left standing for sufficient time to allow diffusion and reaction of H_2 with the sample until the absorption spectrum ceased to change. This procedure was repeated with different pressures of H_2 and the Raman spectra were recorded. The absorption spectra were monitored before and after each Raman measurement and the relative amounts of reduced and oxidized species were determined from the known absorbance in the visible region.[2a] Since the reduction by controlled pressures of H_2 allows the equilibrium between the oxidized and reduced forms to be adjusted to any composition, it is possile to study the conversion process from the fully oxidized to the fully reduced forms systematically. This is difficult with chemical reduction with sodium dithionite, as quantities in excess of stoichiometric amounts have to be added to the sample and then the reduction rapidly goes to completion.

The Raman spectra at liquid nitrogen temperature for the fully reduced and oxidized forms were obtained with a homemade low-temperature cell. The sample in a small cylindrical cell was covered with a paraffin film and attached to the cold finger of the cryostat. For the measurement of the reduced-state spectra, after evacuation, H_2 gas at $\sim$250 Torr was introduced and sufficient time was allowed for H_2 to diffuse through the paraffin film and react with the sample before cooling the cell by liquid nitrogen.

The Raman spectra were obtained with excitations from the Krypton (Spectra-Physics, Model 164), He/Cd (Kinmon Electric, Model CDR8OMGE), and Argon (NEC, Model GLG 3200) lasers and recorded on a JEOL-400D Raman spectrometer equipped with thermoelectricially cooled RCA 31034A photomultiplier and photon counting electronics. Raman shifts were calibrated with indene and are accurate to better than ± 1 cm^{-1} for well-defined bands. The conventional absorption spectra were recorded with a Hitachi 124S spectrophotometer. All the Raman spectra were recorded on an expanded scale with slow speed. The full widths at half-maximum height (fwhm) of the Raman bands for Cyt-c_3 and Cyt-*c* were measured under similar spectral conditions. In order to separate nearby bands of different symmetry species, polarized spectra were used to measure bandwidths of some overlapping bands.

Results

Most of the oxidation state sensitive RR bands[17] arise above 1200 cm^{-1}, and accordingly, we measured the RR spectra in the 1200–1700 cm^{-1} region for this protein using different excitation lines. Under anaerobic conditions, Cyt-c_3 was photoreduced partially with the 406.7-nm excitation and to a lesser extent with the 441.6-nm excitation.[18] Therefore most of the studies were carried out with 514.5-nm excitation with which there was no evidence of photoreduction. We have detected five distinct reduction states of Cyt-c_3 under controlled pressure of H_2 in our studies. Figure 1A shows a part of the RR spectra of Cyt-c_3 from 1275 to 1445 cm^{-1} while Figure 1B shows the spectra from 1470 to 1670 cm^{-1} in the different states of reduction at different pressures of H_2. In these figures, spectra a corresponds to the fully oxidized and e to the fully reduced states. The characteristic band pairs for the fully oxidized and fully reduced forms arise at 1319, 1315 cm^{-1} (ν_{21}); 1374, 1362 cm^{-1} (ν_4); 1409, 1402 cm^{-1} (ν_{29}); 1506, 1492 cm^{-1} (ν_3); 1566, 1540 cm^{-1} (ν_{11}); 1585, 1587 cm^{-1} (ν_{19}); and 1636, 1619 cm^{-1} (ν_{10}), respectively.[19] It is to be noted that the fully oxidized or reduced forms do not show any splittings of the characteristic RR bands although the bands are broad in both forms.

On the other hand, certain bands of the oxidized as well as of the reduced species show splittings into distinct components in the intermediate states of reduction. Since the intensity of the RR band due to the $\nu_{11}(B_{1g})$ mode at 1566 cm^{-1} was reasonable and this band showed very clearly resolved structure, we give the polarized RR spectra in the 1500 to 1580 cm^{-1} region in Figure 2, although polarized spectra were measured for all the bands in the high-frequency region.

As shown in Figures 1 and 2, clearly resolved structure in the intermediate states was observed with the three pairs of bands associated with the $\nu_3(A_{1g})$, $\nu_{11}(B_{1g})$, and $\nu_{10}(B_{1g})$ modes in both the polarized (parallel and perpendicular) and unpolarized spectra in repeated scans, and the position of the split components in different states of reduction is given in Table I. Further confirmation of the resolved structure was obtained by exciting the RR spectra with the 441.6-nm laser line where the bands due to the ν_3 and ν_{11} modes showed similar structure at different states of reduction. (The intensity of the RR band due to the ν_{10} mode becomes too weak with the 441.6-nm excitation to detect resolved components within a reasonable signal-to-noise ratio.) We could not detect any measurable splittings for the anomalously polarized modes probably due to very small separation of the bands between the oxidized and reduced forms. In the partially reduced states, the reasonably strong band due to the $\nu_4(A_{1g})$ mode at 1373 cm^{-1} develops into a very broad feature and there is an overlapping band at 1367 cm^{-1} which becomes clear in the fully reduced form. This overlap and broadness of the band makes it difficult to observe splitting of this band into individual components in the intermediate states of reduction.

After H_2 gas was removed, the cell was aerated and then evacuated again. The Raman spectrum characteristic of the fully oxidized state was obtained and this cycle could be repeated several times confirming that the redox cycling is a fully reversible process. The reduced species is highly autoxidizable.

The bandwidths of Raman lines appeared broader in the fully oxidized and fully reduced states than in intermediate redox states. In order to check if the unresolved and overlapping bands were

(15) Higuchi, Y.; Bando, S.; Kusunoki, M.; Matsuura, Y.; Yasuoka, N.; Kakudo, M.; Yamanaka, T.; Yagi, T.; Inokuchi, H. *J. Biochem.* **1981**, *89*, 1659.

(16) (a) Yagi, T.; Maruyama, K. *Biochim. Biophys. Acta* **1971**, *243*, 214. (b) Yagi, T. *J. Biochem.* **1970**, *68*, 649.

(17) Spiro, T. G. In *Iron Porphyrins*; Lever, A. B. P., Gray, H. B., Eds.; Addison-Wesley: Reading, MA, 1983; Part II, p 89.

(18) Verma, A. L., et al., to be published.

(19) For mode numbering see: Abe, M.; Kitagawa, T.; Ogoshi, H. *J. Chem. Phys.* **1978**, *69*, 4526.

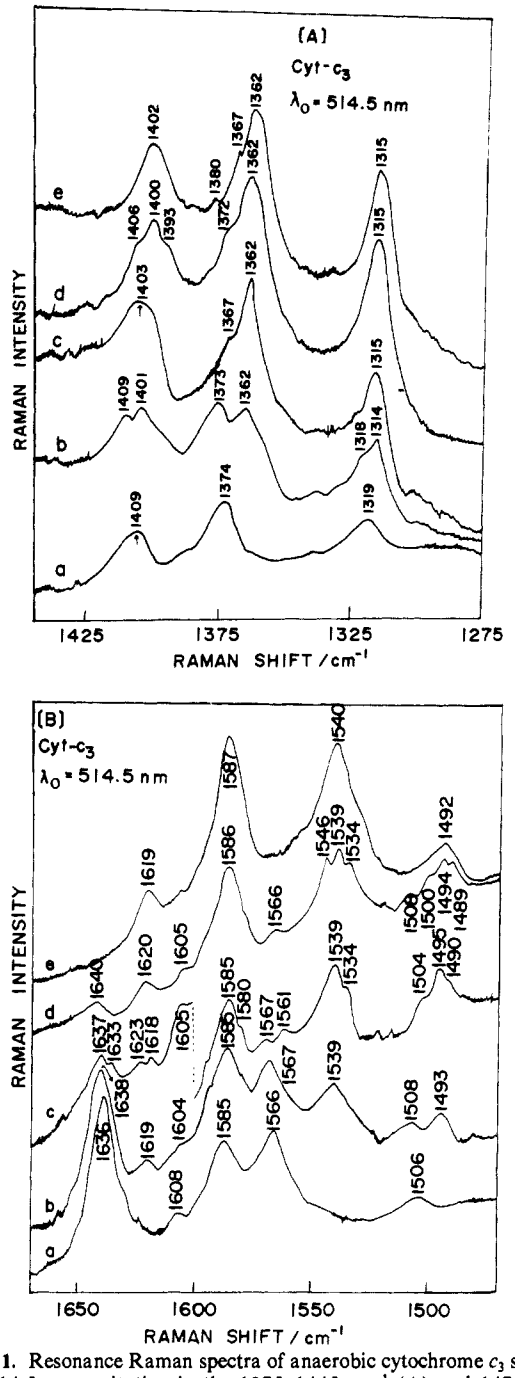

Figure 1. Resonance Raman spectra of anaerobic cytochrome c_3 solution with 514.5-nm excitation in the 1275–1445 cm^{-1} (A) and 1470–1670 cm^{-1} (B) regions. Sample conditions: pH 6.9, $\sim 10^{-4}$ M with a small amount of hydrogenase. Laser: 90 mW at the sample point. Spectrometer: sensitivity, 500 counts/s; scan speed, 5 cm^{-1}/min; time constant, 6.4 s; spectral resolution, 3 cm^{-1}. (a) Fully oxidized; (b) reduction state one; (c) reduction state two; (d) reduction state three; (e) fully reduced form.

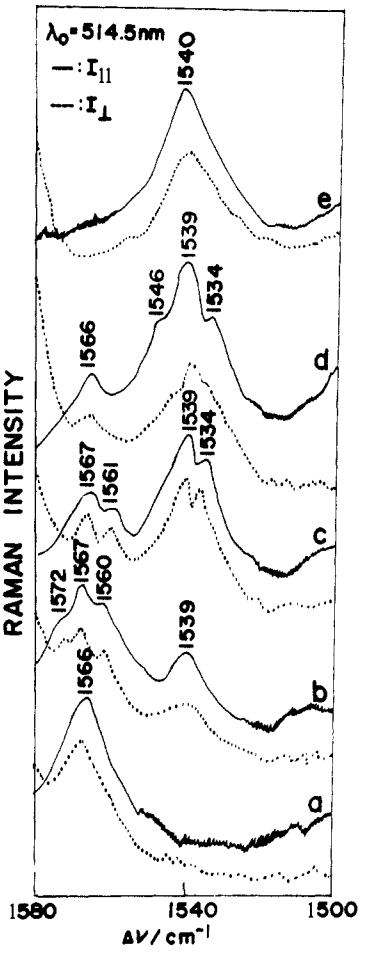

Figure 2. Polarized RR spectra of the anaerobic solution of Cyt-c_3 in the 1500–1580 cm^{-1} region with 514.5-nm excitation. The solid and broken lines represent the parallel and perpendicular polarization components, respectively. The other spectral details are the same as those for Figure 1A except that the spectral resolution here was 3.5 cm^{-1}.

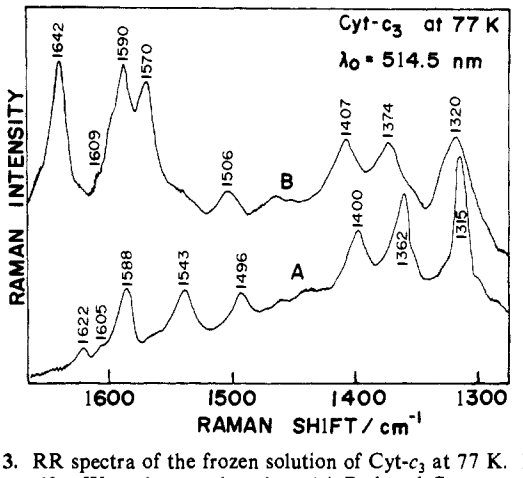

Figure 3. RR spectra of the frozen solution of Cyt-c_3 at 77 K. Laser: 514.5 nm, 60 mW at the sample point. (a) Reduced Cyt-c_3: spectral resolution, 3 cm^{-1}; sensitivity, 500 counts/s. (B) Oxidized Cyt-c_3: spectral resolution, 4.5 cm^{-1}; sensitivity, 250 counts/s.

contributing to the width of the bands at room temperature, we measured the RR spectra of frozen solution of the fully oxidized and reduced forms. Figure 3 shows the RR spectra of Cyt-c_3 for the fully oxidized and reduced forms at liquid nitrogen temperature. We searched carefully but could not detect any splittings for either the oxidized or reduced form, although the bands remained broad even at liquid nitrogen temperature and some bands showed a frequency shift. Further confirmation for the unresolved width of the Raman bands in Cyt-c_3 was provided by comparing their bandwidths with the corresponding Raman lines in Cyt-c where there is only one heme unit. This comparison in Table II under identical spectral conditions clearly shows that the Raman bands of Cyt-c_3 are much broader compared to those of Cyt-c, specially for the band pairs associated with the modes which showed the clearly resolved structures in the intermediate states of reduction.

The observed five distinct reduction states represent primarily the reduction of none, one, two, three, or all four hemes in separate, discrete steps under controlled pressure of H_2. If the electron exchange among the four hemes is much faster than the Raman scattering time, one would expect to observe a time-averaged RR spectrum due to all the forms. On the other hand, slow interconversion would give rise to a simple superposition of the RR

Table I. Frequencies of Some Selected Raman Lines of Cyt-c_3 in Various Redox States[a]

state 0[b]	state 1	state 2	state 3	state 4	mode	symmetry	assignment
		1490	1489				
—	1493	1495	1494	1492	ν_3	A_{1g}	C_aC_m str
			1500				
1506	1508	1504	1508				
		1534	1534				
—	1539	1539	1539	1540			
			1546				
	1560	1561			ν_{11}	B_{1g}	C_bC_b str
1566	1567	1567	1566	—			
	1572						
—	1619	1618	1620	1619			
		1623					
		1633			ν_{10}	B_{1g}	C_aC_m str
1636	1638	1637	1640	—			

[a] Data from the 514.5 nm excited RR spectra for the concentration of 0.1 mM. [b] State number represents approximately the number of the reduced hemes in a single molecule.

Table II. Comparison of Half-Widths (fwhm) of Some Selected Raman Bands for Cyt-c_3 and Cyt-c under Similar Spectral Conditions[a] (cm^{-1})

		oxidized				reduced			
		Cyt-c_3		Cyt-c		Cyt-c_3		Cyt-c	
mode	symmetry	ν	$\Delta\nu_{1/2}$	ν	$\Delta\nu_{1/2}$	ν	$\Delta\nu_{1/2}$	ν	$\Delta\nu_{1/2}$
ν_{10}	B_{1g}	1638	13.3	1635	7.8	1619	10.0	1624	7.2
ν_2	A_{1g}	1585	18.0	1586	11.6	1587	12.5	1585	9.0
ν_{11}	B_{1g}	1566	17.8	1561	11.5	1540	18.0	1547	10.0
ν_3	A_{1g}	1506	16.7	1503	11.6	1492	17.8	1493	11.5
ν_{29}	B_{2g}	1409	14.8	1409	10.6	1402	15.6	1400	10.0
ν_4	A_{1g}	1373	18.9	1372	11.1	1362	14.0	1363	10.9
ν_{21}	A_{2g}	1319	16.0	1318	12.8	1315	12.2	1313	10.0

[a] The band widths ($\Delta\nu_{1/2}$) for the oxidized and reduced forms of both the proteins were measured with a spectral resolution of 4.0 and 1.8 cm^{-1}, respectively, using 514.5 and 441.6 nm excitation lines.

spectra due to the oxidized and reduced species.

Akutsu et al.[7a] and Kimura et al.[7b] recently investigated the NMR spectra of Cyt-c_3 with intermediate redox states and observed a single peak at an intermediate position instead of two peaks at the positions characteristic of the oxidized and reduced forms for methyl protons. Detailed analysis of the position and the width of the observed NMR peaks on the basis of the proposed formulas[20] suggested that the first-order interheme electron exchange in state 1 takes place in ca. 7 ns and that of state 2 occurs in 1 ns.[7b] The second-order rate constant for the electron exchange was obtained by the analysis of the bandwidths of four methyl groups and the values obtained for individual reduction states were all 1×10^4 M^{-1} s^{-1}. Consequently, it was deduced that the intramolecular electron exchange rate is faster ($\sim 10^9$ s^{-1}) while the intermolecular one is slower ($\sim 10^4$ M^{-1} s^{-1}) than the NMR time scale.

In contrast, the observation of well-defined Raman bands due to individual hemes at the characteristic positions for the reduced or oxidized forms indicates that the electron exchange between the reduced and oxidized hemes in each molecule is much slower than the time scale of RR scattering. The Raman scattering time becomes longer under resonance conditions than the nonresonance case. Since the present excitation wavelength is very close to the vibronic band, the scattering time might be as long as picosecond region. Presumably, the residence time of an electron in a particular heme is shorter than 10^{-9} but longer than 10^{-12} s, although the transit time of electrons through protein might be much shorter.

In order to confirm the validity of our conclusions, we measured the RR spectra of cytochrome c (Cyt-c) for which the intermolecular electron exchange between the oxidized and reduced species is known to be slow.[21] The RR spectra in the spectral regions of the ν_3 and ν_4 modes of the partially reduced Cyt-c under controlled amounts of sodium ascorbate are shown in Figure 4

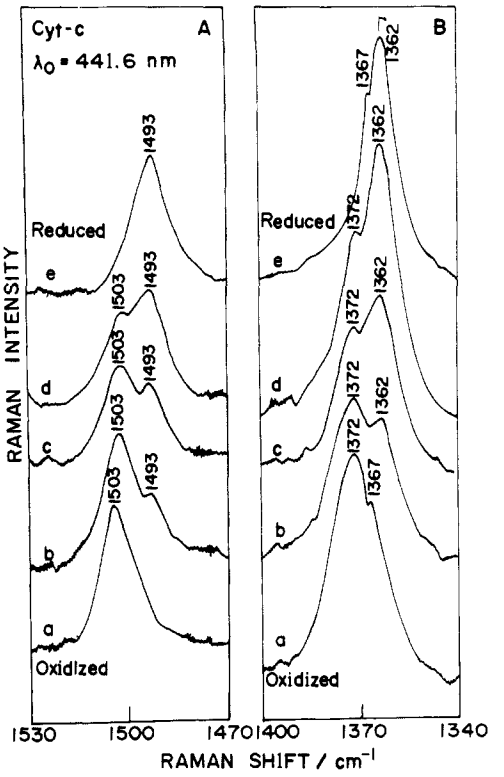

Figure 4. The 441.6 nm excited RR spectra of cytochrome c in 0.1 M phosphate buffer in the spectral regions of the ν_3 and ν_4 modes. The protein with the concentration of 5×10^{-4} M was reduced by controlled amounts of sodium ascorbate with its increasing concentration from a to e. Instrumental conditions: spectral resolution, 3.5 cm^{-1}; sensitivity, 250 counts/s.

where spectrum a is for the fully oxidized and e is for the fully reduced form. As the amount of sodium ascorbate was increased,

(20) Kimura, K. *J. Magn. Reson.* **1983**, *52*, 13.
(21) Gupta, R. K.; Koenig, S. H.; Redfield, A. G. *J. Magn. Reson.* **1972**, *7*, 66.

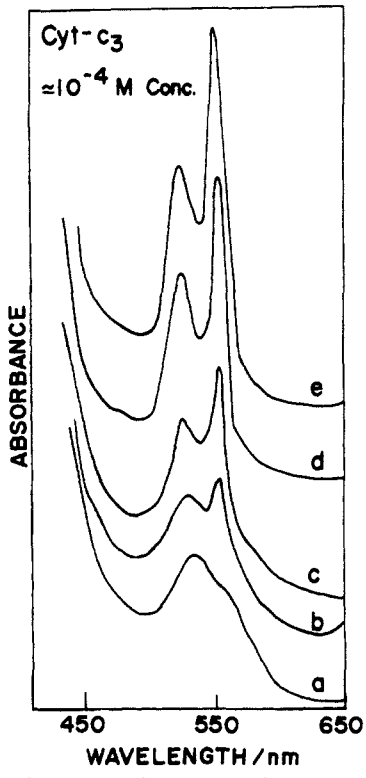

Figure 5. Absorption spectra of the Cyt-c_3 solution in the Q band region. The absorption spectra a to e correspond to the same five reduction states as indicated in Figure 1A. From known extinction coefficient of Cyt-c_3,[13] the percentage of reduced species in the intermediate states of reduction b, c, and d is estimated to be 34, 53, and 78%, respectively, within an accuracy of 5%.

there appeared the partially reduced state for which the well-defined features due to the oxidized and reduced forms are seen at the characteristic positions without any features in between the expected spectral positions for the reduced and oxidized species. These observations suggest the possibility of using the RR technique for probing the electron-transfer processes within biochemical redox proteins.

One may argue about the possibility that the different reduction states of Cyt-c_3 may not correspond to the reduction of individual hemes in discrete steps but to a partial reduction of other hemes along with the reduction of a particular heme and that these partially reduced fractions may also contribute to RR scattering. There is an indication to this aspect as some of the Raman bands in the intermediate states of reduction show slight asymmetry, but the major contribution to the distinct Raman peaks comes from the stepwise reduction of the individual hemes. This feature was clearly demonstrated by the NMR study.[22] Since the RR scattering cross-sections for the oxidized and reduced hemes are quite different, relative Raman intensities cannot be used to determine quantitatively the extent of reduced species. Therefore, we have identified the different reduction states based upon the splittings of the bands into individual components, the required amount of H_2 gas, and the absorption spectra. We monitored the absorption spectra of the protein in the different reduction states as shown in Figure 5, and the intensities of the absorption bands are nearly in conformity with the number of reduced hemes in a particular state. To our knowledge, this is the first observation of clearly resolved splittings of Raman bands free from ambiguities of accidental degeneracies for a multi-heme system.

Discussion

There are two possible ways for interpreting the splittings of Raman bands for a multi-heme protein. One is to assume that each heme is placed in different environments and thus has different vibrational frequencies, and the other is to assume that some heme–heme interactions cause vibrational splitting of equivalent hemes. It is known that when axial ligands are replaced by another amino acid residue for Cyt c through pH changes[23a] or chemical modification,[23b] some Raman bands of heme exhibit a frequency shift even if the protein remains in the low spin state. The most sensitive band reported was ν_{11}.[23b] However, when we compare the ν_{11} frequencies of various C-type cytochromes having a single heme and the histidine and methionine ligands in common, they are not greatly different at neutral pH despite the fact that the amino acid compositions of these proteins and thus heme environments are different from each other: 1561 cm^{-1} for Cyt-c (horse), 1562 cm^{-1} for Cyt-c_2 (*R. rubrum*), 1561 cm^{-1} for Cyt-c 551 (*P. aeruginosa*), and 1563 cm^{-1} for Cyt-c 555 (*C. thiosulphatophilum*).[23a] Therefore, slight differences in heme environments for the hemes with two histidine ligands at axial positions would not be sufficient to cause a large splitting of ν_{11} between 1560 and 1572 cm^{-1} (see state 1 of Table I). Furthermore, the band positions of split components seemed to change with the redox state. For example, the 1506-cm^{-1} band shifts to 1508 cm^{-1} in state 1 and to 1504 cm^{-1} in state 2. Since the spectra were observed in an expanded scale, the 2-cm^{-1} shifts cannot be regarded as errors. If the four hemes were not interacting but were simply nonequivalent, their band positions would not change with the redox state, although their composite might appear differently.

If the four hemes had distinctly different environments, individual hemes would have slightly different absorption maxima and the resultant spectrum of Cyt c_3 as a composite of those four bands should exhibit inhomogeneous broadening. However, the observed half-height full width (Γ) of the Soret band of oxidized (λ_{max} = 410 nm, Γ = 1415 cm^{-1}) and reduced Cyt-c_3 (λ_{max} = 419.5 nm, Γ = 829 cm^{-1}) is appreciably narrower than those of the oxidized (λ_{max} = 409 nm, Γ = 1725 cm^{-1}) and reduced horse heart cytochrome c (λ_{max} = 415 nm, Γ = 1105 cm^{-1}) and the oxidized (λ_{max} = 409 nm, Γ = 1674 cm^{-1}) and reduced beef heart cytochrome c (λ_{max} = 415 nm, Γ = 1161 cm^{-1}). Other single-heme cytochromes c also give rise to a similar bandwidth to those of mammalian cytochrome c as summarized in Table III.[24] Since the absorbance of the α band is about ϵ_{mM} = 28 cm^{-1} $heme^{-1}$ for both Cyt-c_3 and all single-heme Cyt-c's,[13] the narrower bandwidth for Cyt-c_3 implies sharpening of the absorption band, suggesting that the excited energy is rapidly moving among the four hemes.[25] These facts are also unfavorable to nonequivalence of four hemes.

On the other hand, the existence of heme–heme interactions in Cyt-c_3 has been pointed out from the strong dependence of a redox potential of an arbitrary heme on the redox states of other

Table III. The Wavelengths of the Absorption Maxima and the Half-Height Full Widths[24]

	oxidized		reduced	
	λ_{max}/nm	Γ/cm^{-1}	λ_{max}/nm	Γ/cm^{-1}
horse heart Cyt-c	409	1725	415	1105
beef heart Cyt-c	409	1674	415	1161
bacterium Cyt c-553[a]	410	1666	416.7	1093
bacterium Cyt c-555[b]	411	1539	417	1208
bacterium Cyt-c_3	410	1415	419.5	829

[a] From the same strain as that for Cyt-c_3 (*Desulfovibrio vulgaris*, Miyazaki) (from ref 24c). [b] From *Chlorobium thiosulphatophilum* (from ref 24b).

(22) Kimura, K.; Nakajima, S.; Niki, K.; Inokuchi, H. *Bull. Chem. Soc. Jpn.* **1985**, *58*, 1010.

(23) (a) Kitagawa, T.; Ozaki, Y.; Teraoka, J.; Kyogoku, Y.; Yamanaka, T. *Biochim. Biophys. Acta* **1977**, *494*, 100. (b) Ikeda-Saito, M.; Kitagawa, T.; Iizuka, T.; Kyogoku, Y. *FEBS Lett.* **1975**, *50*, 233. (c) Kitagawa, T.; Kyogoku, Y.; Iizuka, T.; Ikeda-Saito, M.; Yamanaka, T. *J. Biochem.* **1975**, *78*, 719.

(24) (a) The absorption spectra of Cyt-c_3, horse and beef cytochromes c, were measured in the present study and, therefore, the half-height full widths are accurate within ±10 cm^{-1}. However, the spectra of bacterial cytochromes c-553 and c-555 were reproduced in an expanded scale from those reported (ref 24b and 24c) and the bandwidths were determined from them in the same way as for Cyt-c_3. (b) Yamanaka, T.; Okunuki, K. *J. Biochem. (Tokyo)* **1968**, *63*, 341–346. (c) Yagi, T. *Biochim. Biophys. Acta* **1979**, *548*, 96–105.

(25) Sumi, H. *J. Phys. Soc. Jpn.* **1972**, *32*, 616–628.

hemes.[7a] Any interaction between the nearby hemes would mix the vibrational modes of the different hemes if they have an identical frequency and split them into four components. This heme–heme interaction would also shift the position of the RR bands compared to the noninteracting environment. As the four heme units in Cyt-c_3 are located at different distances from each other with asymmetric orientations,[15] all four split components may become allowed in Raman scattering. Depending upon the separation between the split components and the half-width of individual components, this structure may be resolved under certain conditions.

In the fully oxidized or reduced forms, all four components would contribute to the Raman scattering, and because of the large intrinsic width of the individual components, one would sample the envelope of these, giving a broad feature without any detectable splitting. However, in the partially reduced state, the RR bands due to the oxidized and reduced species fall in different spectral regions, the number of vibrationally interacting hemes is reduced, and the vibrational coupling is changed. This may facilitate observation of individual components due to the smaller number of interacting hemes resulting in reduced excitonic broadening. Indeed, the structure becomes well resolved in the reduction state 2 (c in Figures 1 and 2) when nearly two hemes are reduced. Our results can be reasonably interpreted in this framework, which may be called vibrational exciton coupling,[26] although the other interpretation cannot be completely ruled out.

The physical processes that may promote the vibrational coupling between the different heme units are of special interest. The total Hamiltonian for a vibrating polyatomic molecule and interacton with its neighbors can be written as[27]

$$H = H_{osc} + H_B + H' \quad (1)$$

where H_{osc} is the Hamiltonian for non-interacting identical oscillators, H_B is the Hamiltonian for the rotational and translational modes of the whole heme group (the "bath"), and H' is the interaction Hamiltonian that couples the internal vibrational coordinates q_i of different hemes to one another and to the "bath" modes, The interaction Hamiltonian, which is modulated by the internal vibrations, can be expanded in a Taylor series of normal coordinates as

$$H' = (\partial V_{ij}/\partial q_i)_0 q_i + \tfrac{1}{2}\sum(\partial^2 V_{ij}/\partial q_i\,\partial q_j)_0 q_i q_j + \ldots \quad (2)$$

where V_{ij} is the interaction energy between the ith and jth hemes ($i, j = 1$–4), and q_i and q_j refer to the same vibrational modes of hemes i and j, respectively. The first term and the diagonal part of the second term in eq 2 induce static frequency shift but not splitting of the unperturbed modes[28] and are expected to make a contribution to the line width. It is the off-diagonal elements of the last term in eq 2 that allow the resonant energy transfer between the same type of normal modes of different hemes and thus may produce splitting of the bands.[28]

The vibrational resonance coupling may originate from a variety of intermolecular forces.[29–31] Depending on the origin of the intermolecular interactions, V_{ij} for interacting hemes can be expressed in the conventional mathematical forms.[32] Nevertheless, our attempts to calculate the magnitude of the splittings due to various interaction terms failed as we could not obtain required parameters such as the magnitude of multipole-moments and their derivatives. Therefore, on the basis of our observations, relative importance of different interaction terms shall be discussed.

Since the iron atom in all the hemes in Cyt-c_3 adopts a low spin state with two identical axial ligands, i.e., histidine, the heme is considered to adopt the planar structure. Accordingly, nearly D_{4h} symmetry can be assumed for the skeletal vibrations of the individual hemes. The observed Raman spectra and polarization properties can be satisfactorily interpreted under this approximation; the resonance enhancement of Raman intensity is expected for the modes of the A_{1g}, A_{2g}, B_{1g}, and B_{2g} species in which the A_{1g} and A_{2g} species give the polarized and anomalously polarized bands, respectively, and B_{1g} and B_{2g} species give the depolarized bands. These vibrations are inactive in infrared and have no associated transition dipole moments. Therefore, the dipole–dipole coupling mechanism can be ruled out with certainty as a cause for the splitting of the Raman bands. The facts that the splittings of the same order of magnitude were observed with the modes of different symmetry species and that the band centers for the parallel and perpendicular polarization components were coincident for all the modes including the A_{1g} modes also rule out the dipole coupling mechanism as a contributing factor for the splittings.

For the vibrational band splittings of molecular crystals, the atom–atom repulsive interaction usually predominates over other intermolecular interactions. However, in Cyt-c_3 the splitting is not limited to the vibrations involving displacements of the atoms in the closest contact in nearby hemes, suggesting that the repulsive interaction would not be the sole origin of the heme–heme interaction.

In general, an increase in dispersion forces lowers the vibrational frequency while an increase in repulsive forces yields an opposite effect.[30] The closest system to noninteracting hemes in Cyt-c_3, having a single heme in a polypeptide chain, is Cyt-c in dilute concentrations. A comparison of the resonance Raman spectra of the oxidized and reduced forms of Cyt-c_3 and Cyt-c observed under the same instrumental conditions shows band pairs for the $\nu_3(A_{1g})$, $\nu_{11}(B_{1g})$, and $\nu_{10}(B_{1g})$ modes; at 1506, 1503 cm^{-1}; 1566, 1561 cm^{-1}; 1638, 1635 cm^{-1} for the oxidized forms; and at 1492, 1493 cm^{-1}; 1540, 1547 cm^{-1}; and 1619, 1624 cm^{-1} for the reduced forms of Cyt-c_3 and Cyt-c, respectively. It is interesting to note that in the oxidized form the frequencies of the corresponding modes are higher for Cyt-c_3 compared to those for Cyt-c while the trend is just the opposite in the case of the reduced form. This comparison indicates that the repulsive forces play a significant role in the heme–heme interactions in the fully oxidized form of Cyt-c_3, while in the reduced form, the dispersion forces become more dominant. There is evidence from Mössbauer studies[10] that the average interheme separation is slightly larger in the reduced form compared to the oxidized form. The closer separation between the hemes in the oxidized form of Cyt-c_3 may result in increased repulsive interactions, giving rise to an upward shift in frequencies compared to the Cyt-c case.

In the reduced form the increased separation between the heme units will result in a decrease of the contribution from the repulsive energy and at the same time the contributon from the dispersion

(26) Craig, D. P.; Walmsley, S. H. In *Excitons in Molecular Crystals*; W. A. Benjamin, Inc.: New York, 1968.

(27) Shelby, R. M.; Harris, C. B.; Cornelius, P. A. *J. Chem. Phys.* **1979**, *70*, 34.

(28) If the potential energy associated with a normal mode is expressed as

$$V_i = (1/2)f_{ii}q_i^2 + (\hbar/6)f_{iii}q_i^3$$

where f_{ii} and f_{iii} are the harmonic and anharmonic force constants, respectively, the separation between the frequencies of the coupled oscillators due to interactions is proportional to[29,30]

$$\nu_1 - \nu_2 \propto (\partial^2 V_{ij}/\partial q_i\,\partial q_j)_0$$

The static frequency shift of a mode due to interactions is

$$\Delta\nu \propto (1/2M\nu_i)[-(3f_{iii}/f_{ii})(\partial V_{ij}/\partial q_i)_0 + (\partial^2 V_{ij}/\partial q_i\,\partial q_j)_0]$$

where M is a reduced mass for the mode.

(29) Dows, D. A. *J. Chem. Phys.* **1960**, *32*, 1342.

(30) McHale, J. L. *J. Chem. Phys.* **1981**, *75*, 30.

(31) Maitland, G. C.; Rigby, M.; Smith, E. B.; Wakeham, W. A. In *Intermolecular Forces*; Oxford University Press: Oxford, 1981.

(32) Various intermolecular interactions are represented as follows:

$$V_{\text{dipole–dipole}} = -(\mu_i\mu_j/\epsilon R_{ij}^3)\phi_1$$

$$V_{\text{quadrupole–quadrupole}} = -(Q_iQ_j/\epsilon R_{ij}^5)\phi_2$$

$$V_{\text{induction}} = -[(\alpha_i\mu_j^2 + \alpha_j\mu_i^2)/(\epsilon^2 R_{ij}^6)]\phi_3$$

$$V_{\text{dispersion}} = -(3\alpha_i\alpha_j/2n^4R_{ij}^6)[I_iI_j/(I_i + I_j)]\phi_4$$

$$V_{\text{repulsion}} = a\exp(-bR_{ij})$$

where α, μ, Q, and I are the polarizability, dipole moment, quadrupole moment, and ionization potential of the heme, respectively, ϕ_i's are the orientation factors, R_{ij} is the effective distance between the ith and jth hemes, and ϵ and n are the dielectric constant and refractive index in the protein.

energy will increase significantly due to much higher RR scattering intensity of the reduced form which implied a larger magnitude of $(\partial\alpha/\partial q)^2$ and thus larger dispersion-induced frequency shifts. The combined effect of these changes in repulsive and dispersion energies may result in a low-frequency shift of the Raman bands in the reduced form of the Cyt-c_3 compared to the Cyt-c. As the contribution of the induction term to the interaction energy depends on the dipole moment, it is expected to be much smaller than the dispersion term for nearly D_{4h} symmetry of individual hemes. Therefore, we conclude that the dispersion and repulsive terms contribute predominantly in the heme–heme vibrational coupling in Cyt-c_3.

The earlier attempts to detect vibrational coupling in the μ-oxo and μ-nitrido dimers of iron protoporphyrin[33] and μ-oxo dimer of iron tetraphenylporphyrin[34] were unsuccessful. Since most of these investigated dimers possess D_{4d} symmetry[35a,b] one could expect to observe only the in-phase component of vibrations of the two hemes in Raman scattering even if there were splittings of modes due to vibrational interactions. Although hemoglobin has four hemes in a molecule, each heme is surrounded by different polypeptide chains and direct heme–heme interaction cannot be expected. Cytochrome oxidase has two heme groups in a protein with different spin states and therefore vibrational coupling may not be detected. To our knowledge, other multi-heme systems have not been examined so carefully, specially with regard to the line width of Raman bands vis-ă-vis their corresponding monoheme systems.

Summarizing the above discussion, we have shown that the RR technique can be used, in suitale situations, to detect vibrational coupling in a multiheme system and to probe the electron-transfer process in redox proteins. The repulsive and dispersion interactions contribute predominantly for the heme–heme interaction in Cyt-c_3. Our conclusions about heme–heme interactions are also supported by an observation of exciton splitting of the Soret band in circular dichroism,[4] Mössbauer,[10] and other studies.[13]

Acknowledgment. The authors thank Drs. H. Akutsu and K. Niki for providing us their NMR results prior to publication.

Registry No. Cyt-c_3, 9035-44-3; heme, 14875-96-8.

(33) Hoffman, J. A., Jr.; Bocian, D. F. *J. Phys. Chem.* **1984**, *88*, 1472.
(34) Adar, F.; Srivastava, T. S. *Proc. Natl. Acad. Sci. U.S.A.* **1975**, *72*, 433. (b) Burke, J. M.; Kincaid, J. R.; Spiro, T. G. *J. Am. Chem. Soc.* **1978**, *100*, 6077.
(35) (a) Scheidt, W. R.; Summerville, D. A.; Cohea, I. A. *J. Am. Chem. Soc.* **1976**, *98*, 6623. (b) Hoffman, A. B.; Collins, D. M.; Day, V. W.; Fleischer, E. B.; Srivastava, T. S.; Hoard, J. L. *J. Am. Chem. Soc.* **1972**, *94*, 3620.

Magnetic Properties in Terms of Localized Quantities. 9. The DNA Bases and the Protonation of Adenine

Michael Schindler

Contribution from the Lehrstuhl für Theoretische Chemie, Ruhr-Universität Bochum, D4630-Bochum, West Germany. *Received December 16, 1987*

Abstract: Chemical shift tensors and magnetic susceptibilities are calculated for some purine and pyrimidine bases by means of the IGLO method. The molecules studied are cytosine, uracil, thymine, adenine, and guanine. Protonation shifts of the ^{13}C and $^{14,15}N$ NMR spectra are calculated for adenine, protonated at N-1, N-3, and N-7. From a comparison with experimental data it is concluded that the second protonation site of adenine is N-3, N-7 being only marginally involved. It is demonstrated that double-ζ basis sets are sufficient only for the calculation of ^{13}C shifts, whereas triple-ζ plus polarization sets are necessary to achieve good agreement with experimental data for nitrogen (and oxygen) NMR shifts.

I. Introduction

Together with the two pentoses 2-desoxy-D-ribose and D-ribose, and with phosphoric acid, the pyrimidine bases thymine (T) (**1**), cytosine (C) (**2**), and uracil (U) (**3**) and the purine bases adenine (A) (**4**) and guanine (G) (**5**) are the essential constituents of the nucleic acids RNA and DNA. Hydrogen bonds between the pairs A-T and G-C are responsible for the helical structure of DNA.

The biochemical and pharmaceutical importance of the nucleobases is a challenge to theory to gain a more than qualitative insight into their spectroscopic properties. Nuclear magnetic resonance spectroscopy (^{13}C, $^{14,15}N$, ^{17}O) has become an extremely powerful tool for the elucidation of complex molecular structures and dynamical processes within the last few years. On the theoretical side gradient techniques facilitate the ab initio geometry optimization of medium sized molecules at the Hartree–Fock level.

However, ab initio calculations of magnetic properties like susceptibilities or NMR chemical shifts for molecules of this size have been very rare. This is due to the fact that conventional theories using one single gauge origin for the external magnetic field suffer from the lack of gauge invariance, i.e., magnetic properties, calculated with finite basis sets, are strongly dependent on the choice of the origin for the vector potential describing the external magnetic field. Even for small molecules large basis sets are necessary to arrive at results that are sufficiently invariant, but for the molecules of this study it is impossible to use methods with one common vector potential.

These computational difficulties have been overcome by the IGLO method.[1] (IGLO stands for *i*ndividual *g*auge for *l*ocalized molecular *o*rbitals.) We have applied it rather successfully to a number of different types of molecules and problems,[2,3] and in this paper we investigate the NMR chemical shift tensors for molecules **1–5**.

Up to now, the consecutive steps, i.e., investigations—on the same level of accuracy—of the pairs A-T and G-C as well as a study of the nucleosides corresponding to the bases **1–5** are beyond our possibilities. What we are intending to do in the near future is to calculate the NMR protonation shifts of all DNA bases. In the present paper we report on protonation effects in adenine **4**.

To give an example for the tremendously increasing demand in CPU time and peripheral storage, we estimate that one A-T or G-C IGLO calculation would require roughly 100 h of billing units at a CDC 205 vectorcomputer with 2MW core storage, and 10^9 two-electron integrals would have to be stored or recomputed in each iteration cycle. Vectorcomputers of the next generation,

(1) Schindler, M.; Kutzelnigg, W. *J. Chem. Phys.* **1982**, *76*, 1919.
(2) Schindler, M. *J. Am. Chem. Soc.* **1987**, *109*, 1020–1033.
(3) Fleischer, U.; Schindler, M.; Kutzelnigg, W. *J. Chem. Phys.* **1987**, *86*, 6337–6347.
(4) Huzinaga, S. Approximate Wave functions, University of Alberta, 1971.

0002-7863/88/1510-6623$01.50/0